Design and Tests of the Injector Synchrotron Magnets for the 7-GeV Advanced Photon Source*

K. Kim, S. H. Kim, K. M. Thompson, and L. R. Turner
Argonne National Laboratory
9700 S. Cass Avenue
Argonne, Illinois 60439

Abstract

Design and magnetic measurements of the pre-production dipole, quadrupole and sextupole magnets for the 7-GeV Advanced Photon Source (APS) injector synchrotron (IS) are described.

I. INTRODUCTION

The APS injector synchrotron requires 68 dipole, 80 quadrupole, and 64 sextupole magnets [1]. The magnets are linearly excited to accommodate the energy of the positron beam between 0.45 GeV and 7 GeV with a ramp time of 0.25 s and an excitation repetition rate of 2 Hz. The main parameters for the three major magnets are listed in Table 1.

Table 1.
Main parameters for major injector synchrotron magnets.

	Dipole	Quadrupole	Sextupole
No. of magnets	68	80	64
Magnetic length	3.077 m	0.5 m	0.12 m
Pole gap	40 mm	56.56 mm	70 mm
Field strength at			
Injection	0.045 T	0.96 T/m	8.8 T/m^2
	(60 A)	(35 A)	(4 A)
Extraction	0.701 T	16.6 T/m	248.0 T/m^2
	(930 A)	(600 A)	(116 A)

The 1.5-mm-thick laminations used for the magnets are of low carbon steel with coercive force less than 1.0 Oe. The laminations are coated on both sides with an epoxy.

The magnet cross sections are symmetrical and designed to allow easy installation of the vacuum chamber by lifting the upper half of the magnets. Pre-production magnets have been fabricated and the required magnetic and mechanical tests completed. The pole-end bevels for dipole and quadrupole magnets have been finalized during the pre-production measurements.

*Work supported by the U.S. Department of Energy, Office of Basic Energy Sciences, under Contract No. W-31-109-ENG-38.

0-7803-1203-1/93$03.00 © 1993 IEEE

II. DIPOLE MAGNET

The cross section of the symmetrical dipole is shown in Figure 1. The laminated steel length of the core is 3.0 m. The top and bottom sections of the magnet are clamped together with bolts on both sides. The required tolerances for quadrupole and sextupole coefficients at a radius of 25 mm are 5×10^{-4} and 1.2×10^{-3}, respectively.

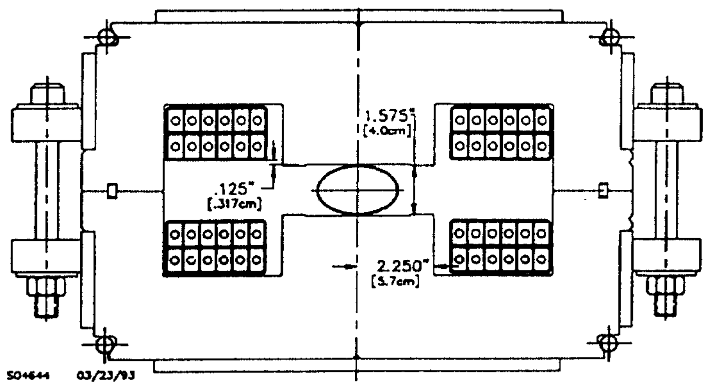

Figure 1. Cross section of the dipole magnet.

The integrated field strength and field variation with transverse displacement are measured using 3.5-m-long curved coils [2]. The integrated and 2-D field shapes at the extraction energy are plotted in Figure 2. The field variations with the transverse displacement of ±25 mm at the injection and extraction fields are less than 2.5×10^{-4} and 1.5×10^{-4}, respectively. From the least square fitting of the measured data within ±30 mm transverse position, the quadrupole and sextupole coefficients at 25 mm are calculated as 0.5×10^{-4} and -0.7×10^{-4}, respectively.

The pole-end bevels are designed so that the integrated and 2-D field shapes are not significantly different, as shown in Figure 2. The end field shapes are measured with 0.5-m-long coils extending 0.25 m outside the core end. Figure 3 includes the field shapes for two bevel geometries with the solid line showing the measurement data for the final geometry (bevel #2). The integrated field for the 0.5-m-length found from 3-D computations for bevel #2 is shown in Figure 3 as a dashed line [3]. The calculations agree with the measurements to within 0.1%.

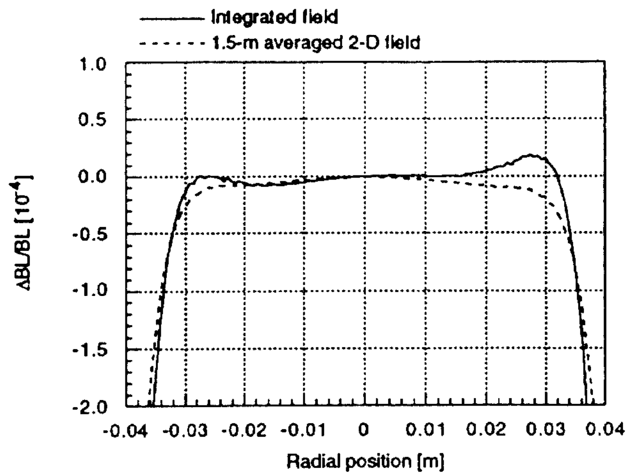

Figure 2. Integrated and 1.5-m averaged 2-D field shape at the extraction energy with respect to the transverse displacement.

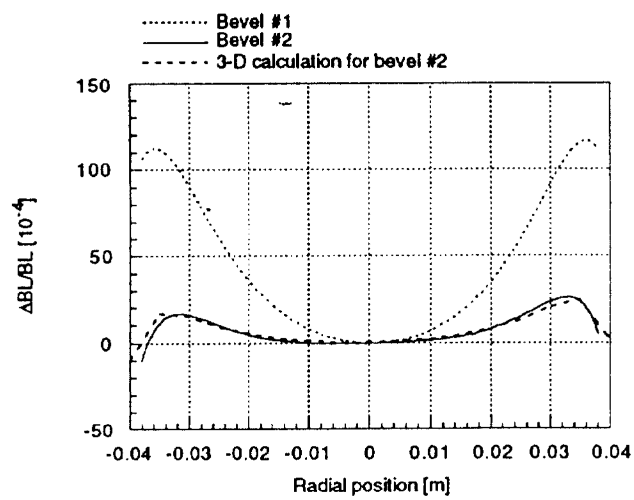

Figure 3. 0.5-m end section field shape at the extraction energy with respect to the transverse displacement.

Table 2.
Description of the data points in Figure 4.

Measurement Number	Remark	$\frac{\Delta BL}{BL}$
1	initially torqued to 150 ft-lb	-1.7×10^{-4}
2	reassembled & torqued to 50 ft-lb	1.0×10^{-4}
3	torqued to 100 ft-lb	0.2×10^{-4}
4	torqued to 150 ft-lb	-0.9×10^{-4}
5	reassembled & torqued to 150 ft-lb	-0.2×10^{-4}
6	reassembled & torqued to 150 ft-lb	0.3×10^{-4}
7	measurement repeated	0.3×10^{-4}
8	reassembled & torqued to 50 ft-lb	1.7×10^{-4}
9	torqued to 100 ft-lb	1.5×10^{-4}
10	torqued to 150 ft-lb	0.7×10^{-4}
11	torqued to 175 ft-lb	-0.7×10^{-4}
12	torqued to 200 ft-lb	-1.7×10^{-4}

In order to assure the field reproducibility of the dipole before and after installation of the vacuum chamber and associated removal of the upper half of the magnet, the dependence of the field integrals on the clamping force of the bolts in Figure 1 were determined. There are 26 bolts on each side of the magnet. Figure 4 shows the reproducibility of the field integrals for several values of the torques on the bolts. The data indicate that clamping at higher torques distorts the magnet geometry. It was indeed confirmed with gap height measurements that larger torques correspond to increases in gap height and decreases in field integral. Repeatability of the field integral is best achieved within 0.7×10^{-4} at a lower torque of 50 ft-lb.

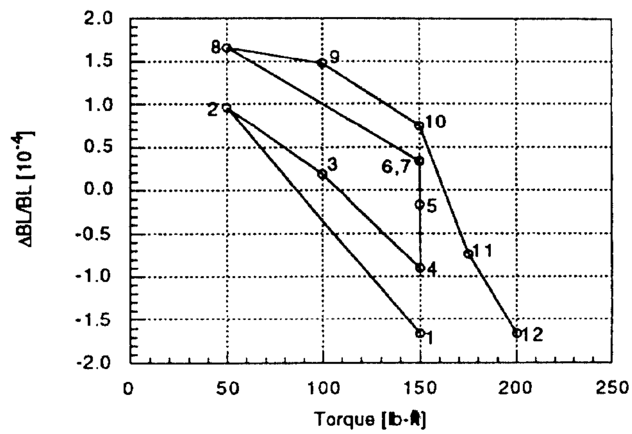

Figure 4. Variation of the dipole field integrals with bolt clamping torques at the extraction energy. (See Table 2 for descriptions of the data points.)

III. QUADRUPOLE AND SEXTUPOLE MAGNETS

The cross sections of the quadrupole and sextupole magnets are shown in Figure 5 (a) and (b). The quadrupole magnet has pole-end bevels of a 30°-cut on five laminations. The magnetic lengths of the quadrupole and sextupole are 0.5 m and 0.12 m, respectively.

A rotating coil system is used for the magnetic measurements [2]. The measurements are conducted when the rotation coil is aligned to the magnetic axis. The radii of the probe coils for quadrupole and sextupole are both 25 mm.

Relative multipole coefficients of the quadrupole magnet at a radius of 25 mm are shown in Figure 6 at four different excitation currents. The skew and other normal coefficients less than 1×10^{-4} are not included here. There are relatively small variations with current. Since the rotating coil axis is aligned to the magnetic axis, the dipole component, which is not shown in Figure 6, is zero. Since the two poles in each lamination are accurately located, the sextupole component is negligibly small. The bevels increased b_5 (dodecapole) by 27.0×10^{-4} with respect to an unbeveled case, while decreasing b_9 (20-pole) by 3.1×10^{-4}.

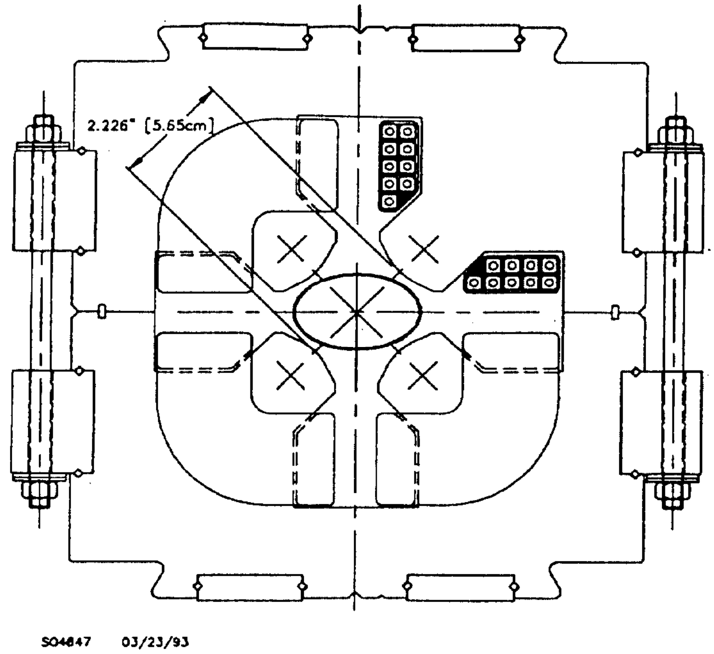

(a) quadrupole

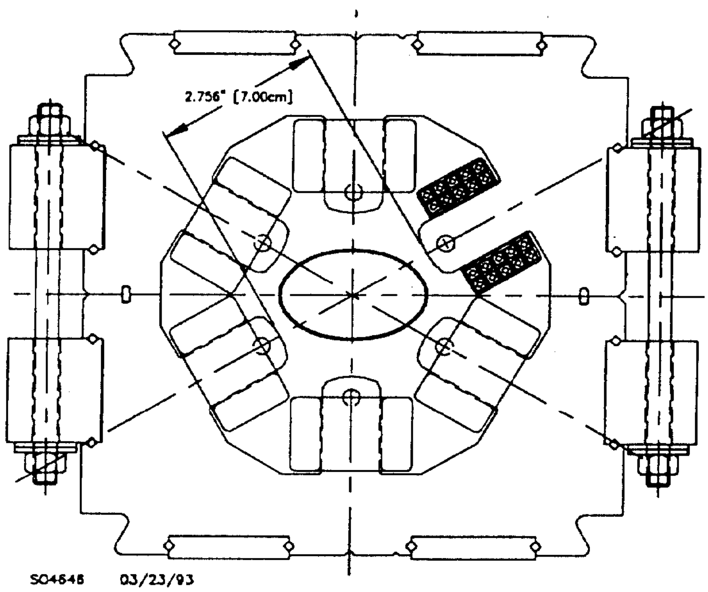

(b) sextupole

Figure 5. Cross sections of the magnets

The multipole coefficients of the sextupole are shown in Figure 7. The magnet does not have pole-end bevels, which makes b_8 a relatively large negative value. Since the rotating coil axis is aligned to the magnetic axis, the quadrupole coefficient b_1 vanishes. The measured dipole field of the magnet was less than 0.1 G.

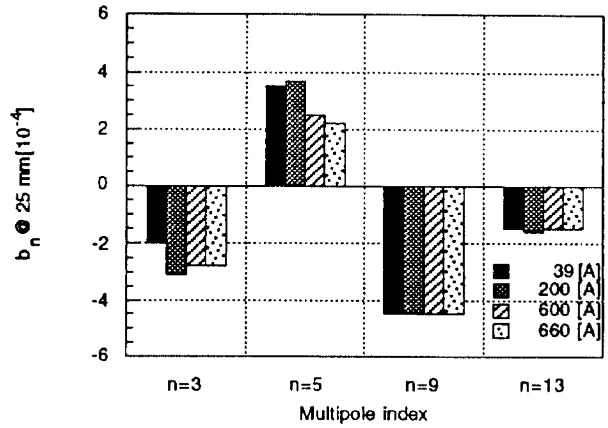

Figure 6. Multipole coefficients of the quadrupole at four different currents. (Index 3 is the octupole coefficient.)

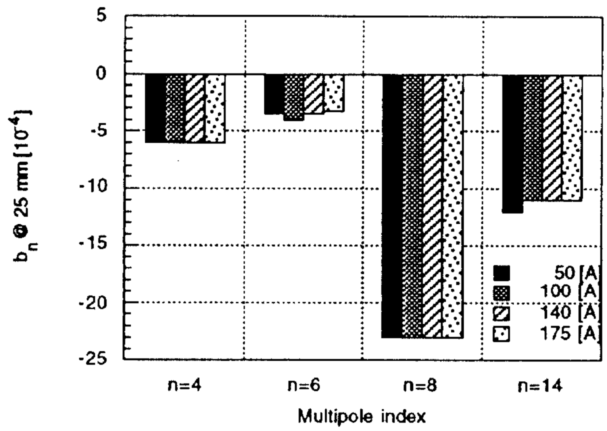

Figure 7. Multipole coefficients of the sextupole at four different currents.

IV. CONCLUSION

By choosing correct geometries for the laminations and pole-end bevels, the integrated field shape of the dipole magnet is flat within 2.5×10^{-4} in the required field region. Clamping force between the top and bottom sections of the magnet was optimized to reproduce the field strength to within 0.7×10^{-4}. The geometry of the pole-end bevel for the quadrupole was selected with the multipole measurements. Multipole coefficients of the quadrupole and sextupole magnets satisfy the required field qualities.

V. REFERENCES

[1] "7-GeV Advanced Photon Source Conceptual Design Report," Argonne National Laboratory, ANL-87-15, 1987.

[2] S. H. Kim, K. Kim, C. Doose, and R. Hogrefe "Magnet Measurement Facility for the 7-GeV Advanced Photon Source," these proceedings.

[3] L. R. Turner, S. H. Kim, K. Kim, and L. Kettunen, "3-D Field Computations for Accelerator Magnets Using Finite Element and Integral Codes," *1992 Int. Conf. on Electromagnetic Field Prob. and Appl.*, Oct. 14-16 1992.